A photothermal microscopy investigation of carrier transport in ion implanted silicon thin films under the action of external electric field

M. NESTOROS*, M. MOUROUTI[a], N. C. PAPANICOLAOU[b], C. CHRISTOFIDES[a]
Department of Electrical and Computer Engineering, University of Nicosia, 1700 Nicosia, Cyprus
[a]*Department of Physics University of Cyprus, 1678 Nicosia, Cyprus*
[b]*Department of Computer Science, University of Nicosia, 1700 Nicosia, Cyprus*

A series of ion implanted Si thin film pseudo-devices with various dimensions in the micrometer region was investigated for different values and orientations of an applied external electric field, utilizing photothermal microscopy. The important features of the photothermal signal namely its linearity as a function of the applied electric field as well as the saturation effect are discussed and an one dimensional model is used for a qualitative interpretation of the results. Photothermal microscopy is proved to be a sensitive technique for carrier transport monitoring in microelectronic circuit elements.

(Received April 11, 2011; accepted May 31, 2011)

Keywords: Photothermal microscopy, Carrier transport, Implanted silicon thin films

1. Introduction

Photomodulated Thermoreflectance (PMTR) has been used extensively for the characterization of a variety of implanted materials and layered structures [1-8]. Concerning applications in electronic materials one can mention among others: ion implantation monitoring, annealing kinetics of defects, etch monitoring and carrier lifetime evaluation. The technique is based on the detection of local temperature excursions on the surface of the material under investigation induced by an intensity modulated light beam via the monitoring of the surface reflectance with the aid of another light beam. The non-contact and non-destructive character of the technique as well as the high sensitivity to thermal inhomogeneities, make PMTR an attractive material evaluation technique. The technological trend towards smaller structures in the field of microelectronics creates the need for characterization techniques with improved spatial resolution. Such a technique is PMTR-microscopy (micro PMTR), a variant of PMTR which combines the advantages of the PMTR technique mentioned above, with the various functions of a microscope offering the ability of viewing the sample under test while characterizing it. In addition it offers an improved spatial resolution as compared to the conventional PMTR technique. Much work has been done in the area of characterization of thermal barriers and optoelectronic structures [9-15] with micro PMTR. The understanding of carrier transport in semiconducting thin films is unambiguously of high importance and can be realised through the evaluation of carrier transport properties. In most cases the evaluation is performed on "passive" samples (absence of electric fields) while in some cases the investigation is performed on active samples (under the effect of external field). An example of investigation of the latter type is the work done by Mandelis et.al [15], who investigated the infrared photothermal radiometric (PTR) and photocurrent signal from silicon films under the action of electric field. The aim of this work was to apply the micro-PMTR technique to micron size semiconducting pseudo-devices (ion implanted silicon thin films) under operation (with the application of external electric field) and investigate the PMTR signal and its components (thermal and free carrier) as a function of the orientation and strength of the applied electric field. The carrier transport under the action of the external electric field and its contribution as a heat source were taken into consideration in order to discuss the results.

2. Experimental

The 0.3 μm thin rectangular Si films were deposited on an insulating substrate and separated in groups of different width (30, 50, 100, 250, 500 μm).

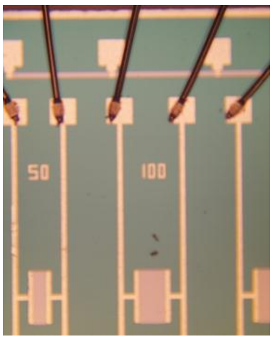

Fig. 1. Part of the circuit at a magnification of 50x showing 50 μm and 100 μm wide thin Si films. At the borders on can see the metal lines as well as five out of the thirty six metal contacts used to apply the external electric field.

A part of the circuit is shown in Fig. 1 at a magnification of 50 X. One can observe a 50 and 100 μm wide thin films with their metal contacts, deposited on the insulating substrate. The electric contacts allow the application of an external electric field along the width of the sample (horizontal direction) and across the thickness of the sample (vertical direction) as shown in Fig. 2. The latter orientation of the electric field is accomplished with the use of a back contact electrode. All samples were ion implanted at a dose of 1×10^{16} P^{+}/cm^{2} and were subject to thermal annealing at 550°C for 30 minutes. The photothermal instrument [15] consists of an Olympus BX51 microscope modified according to the experimental needs and integrated to a standard PMTR setup. An Ar^{+} laser is used as the excitation source and a He-Ne laser as the probe beam source, operating at 488 nm and 632.8 nm, respectively. The excitation beam becomes intensity modulated after passing through a Bragg cell controlled by a frequency generator. The pump and probe beams travel collinearly to the "vertical illuminator" of the Olympus BX51 microscope and then to the "filter tube turret" of the microscope where a selective mirror allows for 95% of the pump beam and 50% of the probe beam intensities to be reflected, by 90 degrees, and directed towards the sample. More details for the setup are presented in the work of Sherifi et. al [15]. The low pump beam intensity on the sample surface (approximately 35 mW for a spot size of 10 μm) results in a low local temperature increase, therefore preserving the non-destructive character of the technique. An external voltage difference from a dc power supply was applied along the width of the samples or along the thickness of the samples by selecting the appropriate contacts. The applied potential difference was varied in steps of a few volts in the range of 0-30 V. A series of micro-PMTR measurements was performed in the modulation frequency range of 1-1000 kHz for different values of the applied voltage difference, for the various samples. A similar series of measurements was also taken for the vertical orientation of the applied electric field.

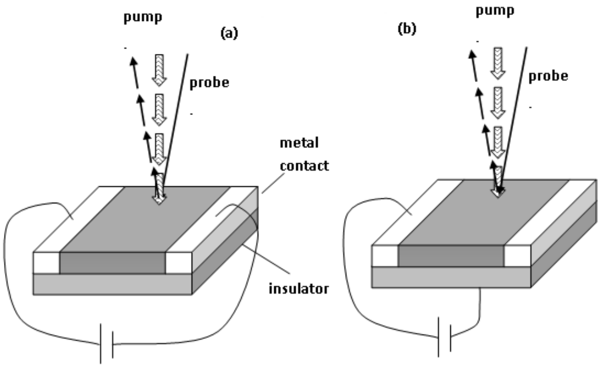

Fig. 2. Experimental setup (a) horizontal orientation of electric field and (b) vertical orientation of electric field.

3. Results and discussion

3.1 Theoretical model and calculations

In order to gain some insight of the problem a one-dimensional model was used to investigate the effect of the external electric field (in the vertical direction) on the PMTR signal. The photoexcited free carrier density is governed by the diffusion equation shown below:

$$\frac{d^2\Delta N(z,\omega)}{dz^2}-\frac{\mu\cdot E}{D}\frac{d\Delta N(z,\omega)}{dz}-\sigma_N^{\,2}\cdot\Delta N(z,\omega)= -\frac{\Phi\cdot(1-R)}{D}\alpha\cdot e^{-\alpha\cdot z} \tag{1}$$

The second term on the left hand side of the above equation is due to the drift of the photoexcited free carriers under the external electric field. The free carrier concentration at depth z at a modulation frequency $f = 2\pi/\omega$ is $\Delta N(z,\omega)$, μ is the mobility of free carriers, E the electric field magnitude, D the carrier diffusivity, α the absorption coefficient of the sample at the excitation wavelength and Φ the incident photon flux. The surface reflectivity at the pump beam wavelength is R. The free carrier wave number is $\sigma_n=(1+ i\cdot \omega\cdot \tau/(D\cdot\tau))^{1/2}$ with τ the free carrier lifetime. The thermal diffusion equation under the intensity modulated photo-excitation takes the form:

$$\frac{d^2\Delta T(z,\omega)}{dz^2}+\frac{E_G}{K\cdot\tau}\Delta N(z,\omega)+\frac{q\cdot\mu\cdot E^2}{K}\Delta N(z,\omega) -\sigma_T^{\,2}\cdot\Delta T(z,\omega)=-\frac{(h\nu-E_G)\cdot\alpha\cdot\Phi\cdot(1-R)\cdot e^{-\alpha\cdot z}}{K\cdot h\nu} \tag{2}$$

where $\Delta T(z,\omega)$ is the local temperature excitation at a depth z and a modulation frequency ω, E_G is the energy gap of the material, K its thermal conductivity, q the electronic charge and $h\nu$ the incident photon energy of the excitation beam. The complex thermal wave number is $\sigma_T = (i\cdot\omega/D)^{1/2}$ with D_T the thermal conductivity. The third term on the left hand side of Eq. (2) is due to Joule heating resulting from the photoexcited free carrier drift under the action of the electric field. The material parameters used for the simulations [5] are typical for amorphous silicon, since the implantation dose is well above the critical amorphization dose [5] and the annealing temperature is not sufficient for recrystallization to take place. The following boundary conditions concerning the photoexcited free carrier concentration and the temperature field were taken into consideration in solving the system of Eqs. (1) and (2)

$$D\frac{d\Delta N(z,\omega)}{dz}\Big|_{z=0}=s_1\cdot\Delta N(z=0,\omega) \tag{3}$$

$$D\frac{d\Delta N(z,\omega)}{dz}\Big|_{z=L}=-s_2\cdot\Delta N(z=0,\omega) \tag{4}$$

$$-K\frac{d\Delta T(z,\omega)}{dz}\Big|_{z=0}=s_1\cdot E_G\cdot\Delta N(z=0,\omega) \tag{5}$$

$$K\frac{d\Delta T(z,\omega)}{dz}\Big|_{z=L} = s_2 \cdot E_G \cdot \Delta N(z=L,\omega) \tag{6}$$

The values of the photoexcited free carrier concentration and temperature excursion at the surface of the sample, *ΔN(0)* and *ΔT(0)* are needed in order to evaluate the PMTR signal according to the familiar expression:

$$\frac{\Delta R}{R} = C_N \cdot \Delta N(0) + C_T \cdot \Delta T(0) \tag{7}$$

In the above expression C_N and C_T are the plasma and thermal coefficients respectively.

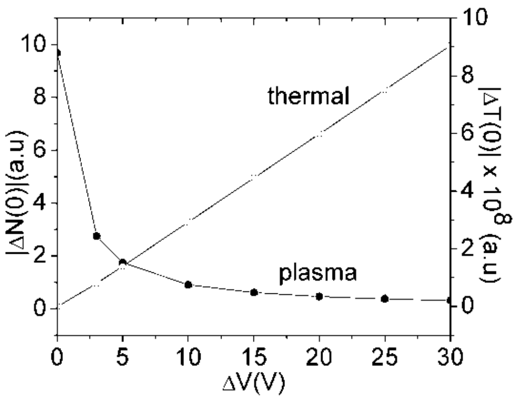

Fig. 3. Simulations of free carrier (plasma) and thermal contribution at the surface, as a function of applied voltage.

The free carrier (plasma) signal component which is proportional to *ΔN(0)* (shown in Fig. 3) decreases with the increase of applied voltage (approximately inversely proportional) since the electric field enhances the diffusion of minority carriers away from the excitation region. In addition *ΔN(0)* shows no variation with the modulation frequency something that is expected since the carrier lifetime used for the simulations (10^{-8} s corresponding to amorphous Si) is too short, relative to the modulation period of the excitation beam. The increase of surface temperature excursion *ΔT(0)* with the applied voltage is expected due to the Joule heating term in Eq. (3) which is proportional to the square of the applied voltage. On the other hand the Joule heating term is also proportional to the free carrier concentration *ΔN* which is decreasing fast with the applied voltage as presented in Fig 3. Furthermore the second term on the right hand side of Eq. (3), which represents the heat source due to carrier recombination, is again proportional to *ΔN*. The antagonistic role of the different terms mentioned above may result in the linear dependence of the thermal component of the signal on the applied voltage, as can be seen from the behavior of the thermal amplitude on the surface *ΔT(0)* calculated for a modulation frequency of 10 kHz (Fig. 3). The simulation showed a dominance of the thermal contribution that masks the free carrier contribution in all simulation scenarios and for both orientations of the applied electric field.

3.2 Experimental results

The experimental micro-PMTR signal amplitude versus modulation frequency presents in all cases (different samples and orientations of the electric field) an increase as the applied voltage increases while the phase channel shows no significant change in the low frequency regime (up to 10 kHz). For higher modulation frequencies the signal phase presents a moderate decrease with the increase of applied voltage. Using the frequency scans for a 30 μm wide circuit with vertical orientation of the applied electric field, a graph (Fig. 4) of the signal amplitude as a function of applied voltage was constructed for different values of the modulation frequency.

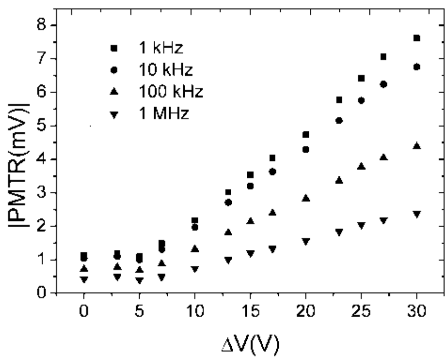

Fig. 4. Micro PMTR amplitude as a function of applied voltage, for a 30 μm wide sample and a perpendicular direction of the applied electric field.

A similar graph (Fig. 5) was constructed for the case of a sample with width of 500 μm and a horizontal orientation of the electric field. In both cases (vertical and horizontal orientation of electric field) one can observe a linear trend of the amplitude above 5V and in the latter case (Fig. 5) a saturation of the signal above 25 V. At this point we have to mention that in their work, Mandelis et. al [16] have shown that the infrared photothermal radiometric (PTR) signal from poly-Si thin films (1 micron) deposited on oxidized n-type Si wafers is proportional to the square of the electric field, while in this work the micro PMTR signal amplitude shows a linear dependence in most cases.

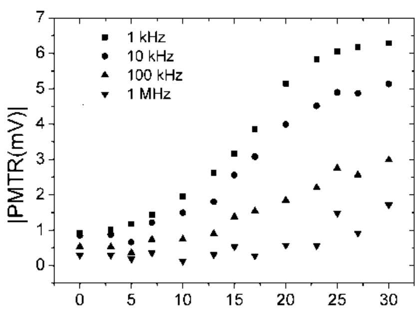

Fig. 5. Micro PMTR amplitude as a function of horizontally applied voltage for various modulation frequencies, in the case of a 500 μm wide sample.

In order to understand the behavior of the micro-PMTR signal as a function of applied electric field one has to take into account how the electric field affects the optoelectronic properties of the material. A very important optoelectronic property is the Shockley-Reed-Hall (SRH) carrier lifetime. The impact of the field enhancement factors of the inverse carrier lifetime was analyzed by Shenk [17] and the carrier lifetime was found to decrease with increasing electric field. Nevertheless according to [17] the carrier lifetime variation with the electric field effect becomes significant at values above 300 kV/cm which were not reached in the present experiments except in the case of the vertically applied field.

One should also consider the impact of the increased dc sample temperature due to Joule heating on the SRH recombination mechanism as was suggested by Mandelis et. al [16]. Nevertheless according to Shenk [17] this temperature variation of SRH carrier lifetime is weak in the range of 300-350 K. Definitely a more detailed model which takes into consideration the temperature dependence of the thermal and electronic transport properties of the samples is needed in order to account such effects.

In the case of the horizontally applied electric field the linearity of the signal amplitude with the applied voltage is distorted for the 250 μm wide sample and it breaks in the case of the 500 μm wide sample (Fig. 5) where it seems to level off (beyond 25 V) for the case of low modulation frequencies (1 and 10 kHz). At a first sight the saturation of the amplitude reminds the saturation of the electric current at high voltages [18] which appears in silicon for electric field values above 2 kV/cm. It is important to say that in the experiments performed the electric field exceeded the critical value mentioned above and reached a value of 100 kV/cm, for the smallest sample (width of 30 microns), without any sign of saturation in the micro-PMTR signal. This indicates that the saturation of the micro-PMTR signal amplitude is not related to a possible saturation of the electric current at high values of electric field.

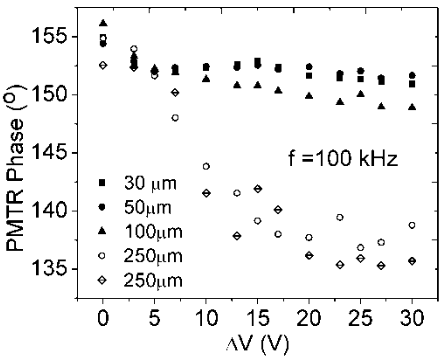

Fig. 6. Micro PMTR phase as a function of horizontally applied voltage for all the samples (various widths).

The signal amplitude saturation beyond 25 V may be due to the polarization effect of the free carriers (electric field induced separation of the photogenerated electron and holes) which leads to a certain increase of the carrier lifetime and the corresponding diffusion length. This means that recombination takes place outside the probe beam area, thus, reducing the signal amplitude. This explanation is supported by the phase channel of the signal. The micro-PMTR signal phase as a function of the applied voltage, for the different samples in the case of horizontally applied electric field at a modulation frequency of 100 kHz, is presented in Fig. 6. In the case of the samples with width that is smaller than 100 μm the phase presents a mild decrease (5^{O}) as the applied voltage increases whereas in the case of the wider samples this decrease in phase is more pronounced (20^{o}). This behavior of the phase channel has to do with the free carrier contribution which becomes more important at high modulation frequencies.

4. Conclusions

The micro-PMTR signal has been proved to be very sensitive to the effect of external electric field applied on ion implanted Si thin films. A linear relation was found to exist between the signal amplitude and the strength of electric field. The saturation of the signal amplitude appearing in the case of horizontal electric fields was attributed to the polarization of free carriers. The saturation phenomenon can be also observed in the phase channel of the signal as a significant decrease of the phase. The micro-PMTR technique can be a useful evaluation tool for the monitoring of carrier transport in microelectronic devices. For this reason it is important to develop the understanding of the dependence of the PMTR signal on the applied electric fields in such structures. More measurements, in combination with a detailed mathematical model, will be performed in the future in order to deduce quantitative results.

References

[1] A. Rosengwaig, J. Opsal, W. L. Smith, D. L. Willenborg, Appl. Phys. Lett. **46**, 1013 (1985).
[2] S. Wurm, P. Alpern, D. M Savignac, R. Kakoschke, Appl. Phys. A. **47**, 147, (1988).
[3] C. Christofides, A. Othonos, E. Loizidou, Appl. Phys. Lett. **82**, 1132, (2003).
[4] A. Salnick, J. Opsal, J. Appl. Phys. **91**, 2874, (2002).
[5] C. Christofides in Ion-Implanted Semiconductors: Optical and Photothermal Characterization Semiconductors and Semimetals, Vol. **46**, ed. C. Christofides, G. Ghibaudo, Academic Press, New York, 115 (1997).
[6] A. Seas, C. Christofides, Appl. Phys. Lett. **66,** 3346, (1995).
[7] G. Benedetto, L. Boarino, R. Spagnolo, Phys. Stat. Solidi A, **146** 777, (1994).
[8] I. A. Vitkin, C. Christofides, A. Mandelis, Appl. Phys. Lett. **54** 2392, (1989).
[9] D. Wawer, T. J. Ochalski, T. Piwoński, A. Wójcik-Jedlińska, M. Bugajski, H. Page, Phys. Stat. Sol. A **202** 1227 (2005).

[10] A. M. Mansanares, J. P. Roger, D. Fournier, A. C. Boccara, Appl. Phys. Lett. **64**, 4, (1994).
[11] A. M. Mansanares, T. Velinov, Z. Bozoki, D. Fournier, A. C. Boccara, J. Appl. Phys. **75,** 3344 (1994).
[12] J. A. Batista, Douglas Takeuti, A. Mansanares, E. C. da Silva, Anal. Sciences 17, s73 (2001).
[13] T. Ikari, J. P. Roger, D. Fournier, Rev. Sci. Instrum. **74,** 553 (2001).
[14] J. Christofferson, A. Shakouri, Microelectronics Journal **35**, 791 (2004).
[15] C. Sherifi, M. D. Papademetriou, M. Nestoros, C. Christofides, Phys. Status Solidi C, **5** 3767 (2008).
[16] A. Mandelis, A. Othonos, C. Christofides, J. Boussey- Said, J. Appl. Phys. **80,** 5322 (1996).
[17] A. Shenk, Solid-State Electron. **35,** 1585 (1992).
[18] K. Seeger, Semiconductor Physics, Springer-Verlag, Berlin, 9th Edition, p.107.

*Corresponding author: mestoros.m@unic.ac.cy